Experimental investigation on the temperature dependence of the nuclear level density parameter

Balaram Dey,[1] Deepak Pandit,[1] Srijit Bhattacharya,[2] K. Banerjee,[1] N. Quang Hung,[3] N. Dinh Dang,[4] Debasish Mondal,[1] S. Mukhopadhyay,[1] Surajit Pal,[1] A. De,[5] and S. R. Banerjee[1,*]

[1]*Variable Energy Cyclotron Centre, 1/AF-Bidhannagar, Kolkata-700064, India*
[2]*Department of Physics, Barasat Govt. College, Barasat, N 24 Pgs, Kolkata-700124, India*
[3]*School of Engineering, Tan Tao University, Tan Tao University Avenue, Tan Duc Ecity, Duc Hoa, Long An Province, Vietnam*
[4]*Theoretical Nuclear Physics Laboratory, Nishina Center for Accelerator-Based Science, RIKEN, 2-1, Hirosawa,*
Wakocity, Saitama 351-0198, Japan
and Institute for Nuclear Science and Technique, Hanoi, Vietnam
[5]*Department of Physics, Raniganj Girls' College, Raniganj-713358, India*

The effect of temperature T and angular momentum J on the inverse level density parameter k has been studied by populating the compound nucleus ^{97}Tc in the reaction ^{4}He + ^{93}Nb at four incident beam energies of 28, 35, 42, and 50 MeV. For all four energies, the value of k decreases with increasing J. The T dependence of k has been compared for two angular momentum windows with different theoretical predictions as well as with the finite-temperature BCS calculation which takes into account the quasiparticle-number fluctuations in the pairing field (FTBCS1). Interestingly, the experimental data are in good agreement with the theoretical calculations at higher J but deviate from all the calculations at lower J.

I. INTRODUCTION

The nucleus is a many-body quantum system which experiences many different configurations even when fairly small excitation energy is provided. It is now a very well-known fact that the density of a quantum mechanical state increases rapidly with excitation energy and soon becomes very large. As a result, the nucleus leaves the discrete region and enters the region of quasicontinuum and continuum. Due to this complexity, statistical concepts and models are not only appropriate but also crucial for comprehension and prediction of various nuclear phenomena. Intriguingly, nuclear level densities are indispensable in the study of nuclear reaction cross sections, nuclear reaction rates [1] which are needed for astrophysical calculations (inputs in modeling stellar evolution and nucleosynthesis), fission or fusion reactor design, transmutation of nuclear waste, and production of radioactive isotopes in therapeutic uses in nuclear medicine. Along with that, they also provide information about thermodynamic quantities such as temperature and entropy as well as pairing correlations in nuclear structure study [2]. The knowledge of nuclear level density is also very crucial while extracting the parameters of giant dipole resonances built on highly excited states of the nuclei [3,4]. However, the characterization of nuclear level density (NLD) in the regions of high excitation energy, angular momentum, and different nuclear shapes is in large part phenomenological. The most commonly used analytical expression for calculating NLD is based on the work of Bethe [5] for a system of noninteracting fermions. The Fermi gas model determines the NLD for a spherical nucleus of mass number A at excitation energy E^* and angular momentum J

and is used in the CASCADE code [4,6,7] as

$$\rho(E^*, J) = \frac{2J+1}{12\mathcal{I}^{3/2}} \sqrt{a} \frac{\exp\left(2\sqrt{aU}\right)}{U^2}. \quad (1)$$

Here $U = E^* - E_{\text{rot}} - \Delta$ is the available thermal energy. E_{rot} is the energy bound in rotation and $\mathcal{I}$ is the effective moment of inertia. The excitation energy is shifted back by the pairing energy Δ which is calculated internally. The NLD parameter a is related to the single-particle level density in the region of the Fermi energy and is correlated to the mass of the nucleus as $a = A/k$, where k is the inverse level density parameter. The temperature dependence of the NLD parameter has been investigated by various theoretical approaches [8–12] and experimental methods [13–17]. It is found from the experimental analysis of nuclear resonances and evaporation spectra that for cold nuclei, $k \sim 8$ MeV; but for high temperatures like $T = 5$ MeV, k is around 13 MeV. The understanding of this behavior has been attempted by taking into account the effects of correlation, i.e., the T dependence of the frequency-dependent effective mass as well as the finite size effect, the momentum dependence of the effective mass, the effects of continuum, and the shell effects [8,11,12].

It may be noted that the level density formalism given in Eq. (1) is for a system of noninteracting fermions with equidistant single-particle states and does not include the collective enhancement of NLD due to the coupling of rotational as well as vibrational degrees of freedom with the single-particle degrees of freedom. The enhanced level density is expressed as $\rho(E^*, J) = \rho_{\text{int}}(E^*, J)K_{\text{coll}}(E^*)$, where $K_{\text{coll}}(E^*)$ is the collective enhancement factor consisting of both vibrational and rotational contributions [18]. Very recently, neutron evaporation spectra from ^{201}Tl*, ^{185}Re*, and ^{169}Tm* compound nuclei have been measured at two excitation energies ($E^* \sim 37$ and 26 MeV) to study the effect of collectivity by extracting the inverse level density parameter k [19]. It was observed that for large ground-state

deformed nuclei (^{185}Re* and ^{169}Tm*) the value of k decreased substantially at the lower excitation energy, while for a near-spherical nucleus (^{201}Tl) it remains the same at the two excitation energies. The results indicated a strong correlation between collectivity and ground-state deformation.

Recently, there have been ample experimental efforts to comprehend the spin dependence of the level density parameter. In a few measurements of angular momentum gated neutron evaporation spectra in $A \sim 119, 97$, and 62, it was seen that the k value decreased with increase in J which indicated that level density increases with J [7,20]. On the other hand, the inverse level density parameter extracted from the α evaporation spectra in the $A \sim 180$ and $A \sim 120$ mass regions showed that the value of k is either constant or increases with angular momentum [21,22]. However, theoretical calculation for similar masses shows that the k value should increase with angular momentum for all the systems [23]. Interestingly, the γ-multiplicity gated proton spectra in $A \sim 105$ showed a drastic dependence on fold. The spectra acquired a broad structure at higher multiplicity folds for proton energies beyond $\sim$15 MeV which was explained by a prescription of a localized enhancement of NLD [24]. Thus, extremely exciting but conflicting experimental results on the spin dependence of the level density parameter motivate one to carry out further investigations.

In this work we report on the angular momentum gated neutron evaporation spectra at different excitation energies (30–50 MeV) for the reaction ^{4}He $+$ ^{93}Nb. The specific advantage of using a light ion reaction is that the major residues are of similar nature and in our case they are ^{95}Tc, ^{94}Tc, and ^{93}Tc depending on the excitation energy of the compound nucleus. However, for excitation energies above 42 MeV, another channel contributes ($\sim$20%) due to ($\alpha, \alpha 2n$) populating ^{91}Nb. Nevertheless, the deformations of all the nuclei populated in the decay chain are similar and are of the order of $\beta \sim 0.05$. The shell effects are also very small and similar. Therefore, the neutron evaporation spectra will have the contribution from similar kind of nuclei only.

II. EXPERIMENTAL DETAILS

The experiment was performed at the Variable Energy Cyclotron Centre, Kolkata, using the α beam from the K-130 cyclotron. A self-supporting 1 mg/cm^2 thick target of 99.9% pure ^{93}Nb target was used. Four different beam (^{4}He) energies of 28, 35, 42, and 50 MeV were used to populate the compound nucleus ^{97}Tc at the excitation energies of 29.3, 36.0, 43.0, and 50.4 MeV, respectively. The maximum populated angular momenta for fusion were 16, 18, 19, and 20 $\hbar$, respectively. The evaporated neutrons from the compound nucleus (CN) were detected by a liquid organic scintillator (BC501A) based neutron detector [25] that was placed at a distance of 1.5 m from the target position and at an angle of 125° to the beam axis. Along with the BC501A neutron detector, a 50-element low-energy γ-multiplicity filter [26] was also used to estimate the angular momentum populated in the compound nucleus as well as to get a fast start trigger for neutron time-of-flight (TOF) measurement. The multiplicity filter was split into two blocks of 25 detectors each, in a

staggered castle type geometry to equalize the solid angle for each multiplicity detector element, and placed at a distance of 5 cm above and below the center of the target. The efficiency of the multiplicity setup was 56% as calculated using GEANT4 simulation. A level-1 trigger (A) was generated from the multiplicity filter array when at least one detector each from the top and bottom blocks fired in coincidence above a threshold of 250 keV. Another trigger (B) was generated when the signal in BC501A detector crossed a threshold of 250 keV. An online coincidence of these two triggers (A and B) ensured the selection of neutron events and rejected the backgrounds. The TOF technique was employed for neutron energy measurement. The neutron-γ ray discrimination was achieved by both pulse shape discrimination (PSD) and TOF techniques. To keep the background of the detectors at a minimum level, the beam dump was heavily shielded with lead bricks and borated paraffin. A CAMAC electronics and VME based data acquisition system were used to simultaneously record the energy and time information of the detectors.

III. DATA ANALYSIS AND RESULTS

The TOF spectrum was converted to an energy spectrum using the prompt γ peak as a time reference. The efficiency correction for the BC501A neutron detector was performed using GEANT4 simulation [27]. In order to extract the inverse level density parameter from the experimental neutron spectra, the theoretical neutron energy spectra were calculated employing the statistical model code CASCADE [6]. The level density parameter prescription of Ignatyuk *et al.* [28] was adopted which takes into account the nuclear shell effects at
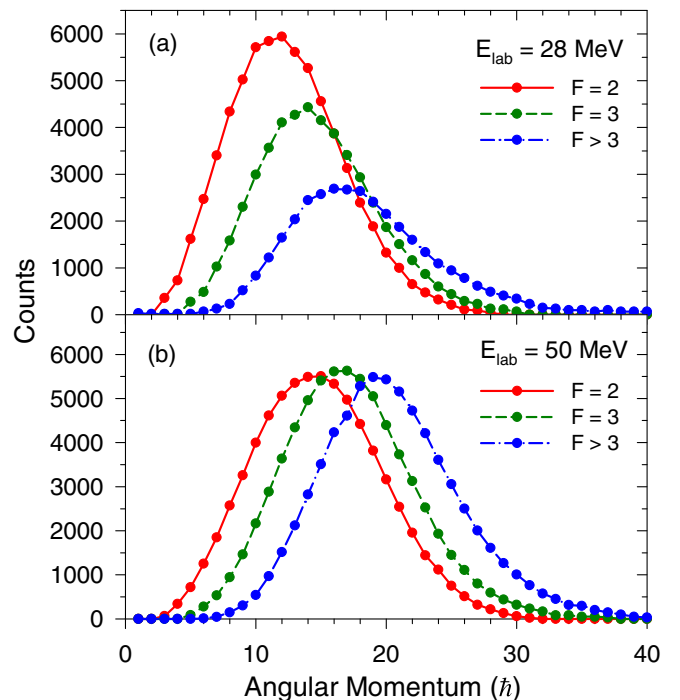

FIG. 1. (Color online) Angular momentum distribution for different folds for the ^{4}He $+$ ^{93}Nb system at 28 and 50 MeV incident energy.
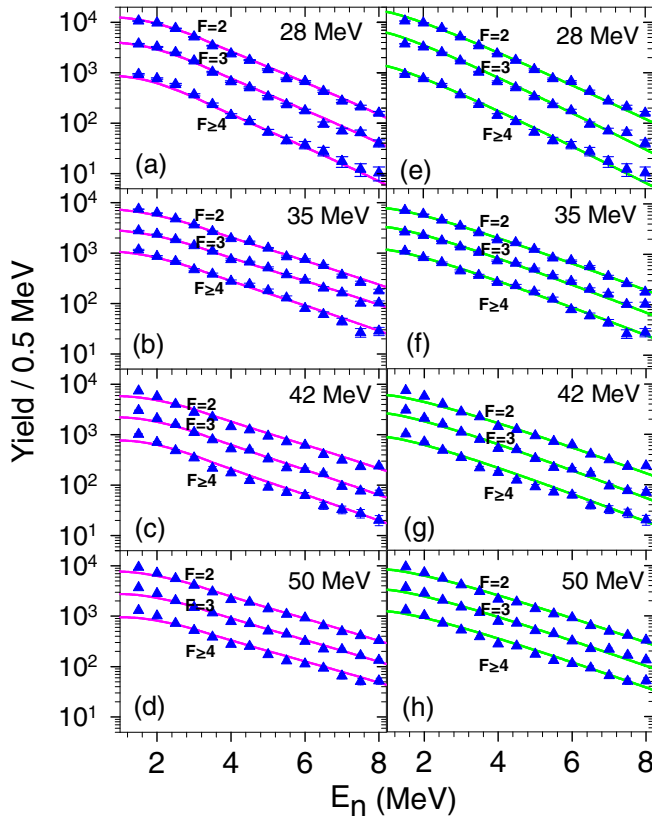
FIG. 2. (Color online) [(a)–(d)] Neutron evaporation energy spectra (filled triangles) along with the CASCADE predictions (continuous line) for different folds (F) at incident energies of 28, 35, 42, and 50 MeV for ^{4}He + ^{93}Nb system. [(e)–(f)] Neutron evaporation energy spectra (filled triangles) along with the Maxwellian fitting (continuous line) for different folds (F) at incident energies of 28, 35, 42, and 50 MeV for ^{4}He + ^{93}Nb system. $F = 2$ and $F = 3$ data have been multiplied by 100 and 10, respectively.

low excitation energy and connects smoothly to the liquid drop value at high excitation energy. The transmission coefficients for statistical calculation were obtained from the optical model. The potential parameters for neutron, proton, and α were taken from Refs. [29], [30], and [31], respectively. The experimental fold distribution measured using the 50-element γ-multiplicity filter was converted to the spin distribution using GEANT4 simulation applying the approach discussed in Ref. [26]. The simulated spin distributions deduced from the experimental fold distributions were used as inputs for different folds. The angular momentum distributions for different folds at 28 and 50 MeV incident energies are shown in Fig. 1. The moment of inertia of the CN was taken as $I_{\text{eff}} = I_0(1 + \delta_1 J^2 + \delta_2 J^4)$, where I_0 is the moment of inertia of the spherical nucleus. The role of the deformation parameters δ_1 and δ_2 was found to be inconsequential and the shapes of the neutron energy spectra were mostly dependent on the inverse level density parameter. The value of k has been extracted from the best-fit statistical model calculations using a χ^2 minimization in the energy range of 3–7 MeV (Fig. 2). The extracted k are given in Table I for different angular momenta and excitation energies.

TABLE I. Average temperature and average angular momentum along with the level density parameter for the ^{4}He + ^{93}Nb system at different beam energies.

System	E^* (MeV)	$\langle J \rangle$ $\hbar$	$\langle T \rangle$ (MeV)	A/k (MeV^{-1})
^{4}He + ^{93}Nb @ E_{lab} = 28 MeV	29.3	12 ± 5	1.18 ± 0.03	$A/(8.5 \pm 0.5)$
		14 ± 6	1.06 ± 0.04	$A/(8.3 \pm 0.3)$
		16 ± 5	1.03 ± 0.02	$A/(8.0 \pm 0.5)$
^{4}He + ^{93}Nb @ E_{lab} = 35 MeV	36.0	13 ± 4	1.47 ± 0.02	$A/(9.7 \pm 0.5)$
		15 ± 5	1.41 ± 0.03	$A/(9.5 \pm 0.3)$
		18 ± 5	1.35 ± 0.04	$A/(8.2 \pm 0.4)$
^{4}He + ^{93}Nb @ E_{lab} = 42 MeV	43.0	14 ± 5	1.52 ± 0.05	$A/(9.0 \pm 0.4)$
		16 ± 5	1.43 ± 0.02	$A/(8.1 \pm 0.4)$
		19 ± 6	1.38 ± 0.04	$A/(7.8 \pm 0.5)$
^{4}He + ^{93}Nb E_{lab} = 50 MeV	50.4	14 ± 5	1.60 ± 0.02	$A/(9.2 \pm 0.5)$
		16 ± 5	1.55 ± 0.02	$A/(8.5 \pm 0.4)$
		20 ± 5	1.50 ± 0.03	$A/(8.2 \pm 0.4)$

It is very interesting to note that the values of k decrease with increasing angular momentum for all the incident energies (Fig. 3). The result is in contrast to the theoretical calculations obtained under the framework of statistical theory of hot rotating nuclei which predicts that k should increase with angular momentum [23]. However, the trend of the angular momentum dependence measured in this work is consistent with the previous measurements for ^{62}Zn [20] and ^{119}Sb [7]. The inverse level density parameter as a function of temperature, for two angular momentum windows, has also been compared with the different theoretical calculations predicted by Shlomo [8], Lestone [9], and Mughaghab [10] (Fig. 4). It should be mentioned that the prediction of Shlomo was taken for the $A = 110$ mass region [8] whereas the other two predictions were calculated for the $A = 97$ mass using the formula given in Refs. [9,10]. Since, the neutron evaporation spectra include neutrons from different nuclei in the decay chain, the average temperatures for different excitation energies were
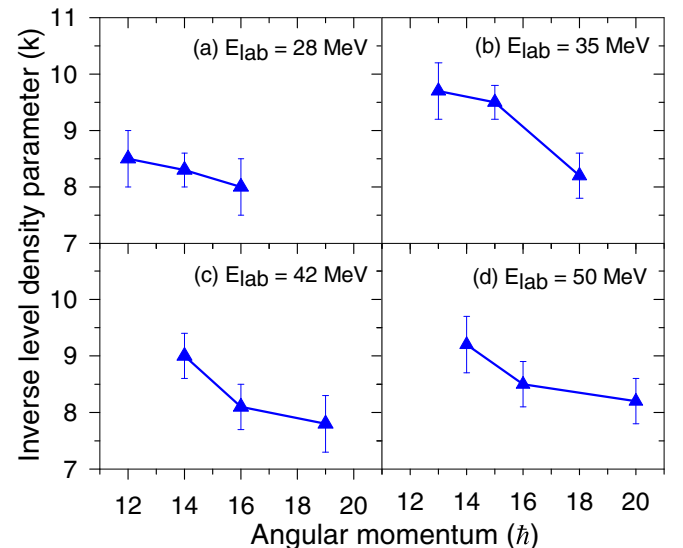

FIG. 3. (Color online) Angular momentum dependence of k at four incident energies.
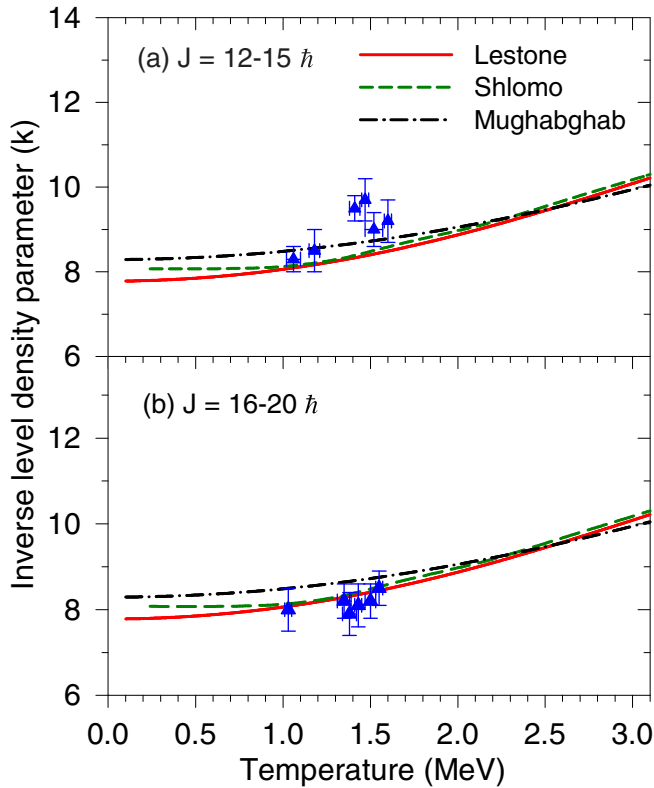
FIG. 4. (Color online) Temperature dependence of k compared with different theoretical calculations.

FIG. 5. (Color online) Temperature dependence of k compared with the calculations of FTBCS and FTBCS1.

calculated by fitting the experimental data with the Maxwellian function $\sqrt{E}\exp(-E/T)$. It needs to be mentioned that none of the theoretical predictions include the J effect. As can be seen from Fig. 4, the inverse level density parameter increases with temperature for all the predictions. However, the data at higher angular momenta match very well with the prediction but are at disparity at lower angular momenta. This outcome was unexpected since the theoretical predictions do not include the J effect and, thus, experimental data and theoretical calculations should have matched at lower J. The results indicate that the level density is suppressed at lower angular momenta. This deviation cannot be attributed to the effect of collectivity because the level density is not enhanced but suppressed compared to the Fermi gas model.

Recently, the temperature dependence of the level density was studied in hot medium-mass nuclei, which undergo a noncollective rotation about the symmetry axis [32]. The numerical calculations within the finite-temperature BCS (FTBCS) and FTBCS1 theories have shown the pairing reentrance in the pairing gap at finite angular momentum M (M is the z projection of total angular momentum) and temperature T. The FTBCS1 theory includes the effects due to quasiparticle-number fluctuations in the pairing field at $T \neq 0$ MeV. Both the FTBCS and FTBCS1 theories take into account the z-projection of angular momentum at $T \neq 0$ MeV. The pairing reentrance changes the T dependence of the level density from a convex function to a concave one. Similar calculation was performed to observe whether the pairing reentrance plays any important role in the case
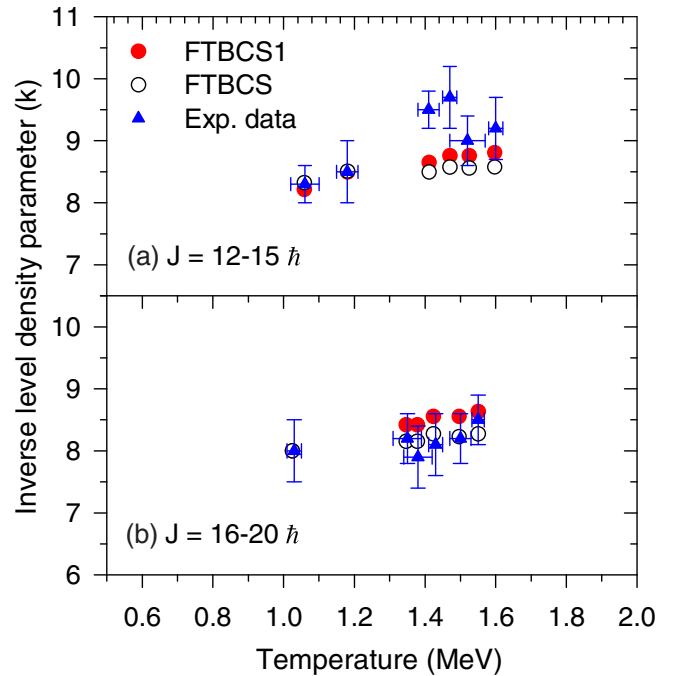
of ^{97}Tc. It was observed that the FTBCS gaps collapse at a certain critical temperature, whereas the FTBCS1 gaps do not. Starting from $M = 12\ \hbar$ the FTBCS1 proton gap shows the pairing reentrance effect, that is, the pairing gap reappears and remains finite at $T > 0.3$ MeV and $M \geqslant 12\ \hbar$. The value of k was extracted from the excitation energies using the relation $k = 4AE^*/S^2$. Since, the nucleus ^{97}Tc is not spherical but slightly prolate and the calculations were carried out under the assumption of a spherical nucleus for which the z projection M of the total angular momentum J coincides with J, the results of theoretical calculations have been renormalized to match the corresponding data point at the lowest J for both the selected angular momentum window. As can be seen from Fig. 5, the increase of k with T observed in the data is also reproduced by the results of theoretical calculations although the latter agree better with the data for the higher J window whereas for the lower J window the theory underestimates the two data points at $T = 1.41$ MeV ($J = 15\ \hbar$) and 1.47 MeV ($J = 13\ \hbar$). The FTBCS and FTBCS1 predict similar results, indicating that pairing reentrance might have a minor effect on the inverse level density parameter in this case. However, to have a thorough understanding of the effect of collectivity and pairing reentrance on the decrease of k with increasing angular momentum, much more theoretical and experimental studies are needed. Moreover, it may be noted that the effect of angular momentum on k is not observed for higher masses [21,22,33] but is only apparent in low- and medium-mass $A \leqslant 120$ nuclei [7,20]. Hence, more experimental data at both high- and low-mass regions are required to understand this behavior.

IV. SUMMARY AND CONCLUSIONS

Angular momentum gated neutron evaporation spectra have been measured in the reaction ^{4}He + ^{93}Nb at $E_{\mathrm{lab}} = 28, 35,$

42, and 50 MeV to study the T and J dependence of the inverse level density parameter k. It was observed that k decreased with increasing J for all excitation energies. The T dependence of k was studied by selecting two angular momentum windows and compared with different theoretical calculations. Intriguingly, the results of all the theoretical calculations agree well with the data at the higher J window but differ from the experimental data at the lower J window.

[1] T. Rauscher, F.-K. Thielemann, and K.-L. Kratz, Phys. Rev. C **56**, 1613 (1997).

[2] E. Melby *et al.*, Phys. Rev. Lett **83**, 3150 (1999).

[3] Balaram Dey *et al.*, Phys. Lett. B **731**, 92 (2014).

[4] S. Bhattacharya, D. Pandit, B. Dey, D. Mondal, S. Mukhopadhyay, S. Pal, A. De, and S. R. Banerjee, Phys. Rev. C **90**, 054319 (2014).

[5] H. A. Bethe, Phys. Rev. **50**, 332 (1936); Rev. Mod. Phys. **9**, 69 (1937).

[6] F. Puhlhofer, Nucl. Phys. A **280**, 267 (1976).

[7] K. Banerjee *et al.*, Phys. Rev. C **85**, 064310 (2012).

[8] S. Shlomo and J. B. Natowitz, Phys. Lett. B **252**, 187 (1990); Phys. Rev. C **44**, 2878 (1991).

[9] J. P. Lestone, Phys. Rev. C **52**, 1118 (1995).

[10] S. F. Mughabghab and C. L. Dunford, BNL-NCS-65712, Conference 981003, 1998 (unpublished).

[11] M. Prakash, J. J. Wambach, and Z. Y. Ma, Phys. Lett. B **128**, 141 (1983).

[12] J. N. De, S. Shlomo, and S. K. Samaddar, Phys. Rev. C **57**, 1398 (1998).

[13] K. Hagel *et al.*, Nucl. Phys. A **486**, 429 (1988).

[14] M. Gonin *et al.*, Phys. Lett. B **217**, 406 (1989); Phys. Rev. C **42**, 2125 (1990).

[15] A. Chbihi *et al.*, Phys. Rev. C **43**, 652 (1991); **43**, 666 (1991).

[16] B. J. Fineman, K.-T. Brinkmann, A. L. Caraley, N. Gan, R. L. McGrath, and J. Velkovska, Phys. Rev. C **50**, 1991 (1994).

[17] D. Fabris *et al.*, Phys. Rev. C **50**, R1261(R) (1994).

[18] A. V. Ignatyuk, K. K. Istekov, and G. N. Smirenkin, Sov. J. Nucl. Phys. **29**, 450 (1979).

[19] P. Roy *et al.*, Phys. Rev. C **88**, 031601(R) (2013).

[20] P. Roy *et al.*, Phys. Rev. C **86**, 044622 (2012).

[21] Y. K. Gupta, D. C. Biswas, B. John, B. K. Nayak, A. Saxena, and R. K. Choudhury, Phys. Rev. C **80**, 054611 (2009).

[22] Y. K. Gupta, B. John, D. C. Biswas, B. K. Nayak, A. Saxena, and R. K. Choudhury, Phys. Rev. C **78**, 054609 (2008).

[23] M. Aggarwal and S. Kailas, Phys. Rev. C **81**, 047302 (2010).

[24] A. Mitra, D. R. Chakrabarty, V. M. Datar, Suresh Kumar, E. T. Mirgule, H. H. Oza, V. Nanal, and R. G. Pillay, Nucl. Phys. A **765**, 277 (2006).

[25] K. Banerjee *et al.*, Nucl. Instrum. Methods Phys. Res., Sect. A **608**, 440 (2009).

[26] D. Pandit, S. Mukhopadhyay, S. Bhattacharya, S. Pal, A. De, and S. R. Banerjee, Nucl. Instrum. Methods Phys. Res., Sect. A **624**, 148 (2010).

[27] S. Agostinelli *et al.*, Nucl. Instrum. Methods Phys. Res., Sect. A **506**, 250 (2003).

[28] A. V. Ignatyuk, G. N. Smirenkin, and A. S. Tishin, Sov. J. Nucl. Phys. **21**, 255 (1975) [Yad. Fiz. **21**, 485 (1975)].

[29] C. M. Perey and F. G. Perey, At. Data Nucl. Data Tables **17**, 1 (1976).

[30] F. G. Perey, Phys. Rev. **131**, 745 (1963).

[31] L. Mcfadden and G. R. Satchler, Nucl. Phys. A **84**, 177 (1966).

[32] N. Quang Hung and N. Dinh Dang, Phys. Rev. C **84**, 054324 (2011).

[33] M. Gohil *et al.*, EPJ Web Conf. **66**, 03073 (2014).